

CORPORATE RESEARCH

EXXON RESEARCH AND ENGINEERING COMPANY • ANNANDALE, NEW JERSEY

**THE FATE OF CO₂ FROM THE NATUNA GAS PROJECT
IF DISPOSED BY SUBSEA SPARGING**

Brian P. Flannery, Andrew J. Callegari
Bahlin Nair, and Wayne G. Roberge

THE FATE OF CO₂ FROM THE NATUNA GAS PROJECT IF DISPOSED BY SUBSEA SPARGING

We investigate the consequences of disposing CO₂ waste gas from the Natuna project by sparging CO₂ into the ocean at 140 m depth near the site. The large reservoir of natural gas discovered near Natuna Island in the South China Sea contains over 70 percent CO₂. Proposed levels of production amount to about 0.4 percent of the current total global CO₂ emissions. This would make Natuna the world's largest point source emitter of CO₂ and raises concern for the possible incremental impact of Natuna on the CO₂ greenhouse problem. While the base case production scheme calls for atmospheric venting of CO₂, an alternative has been proposed in which CO₂ would be sparged into seawater so that, perhaps, CO₂ would never appear in the atmosphere.

Here we develop models for the chemistry and transport of CO₂ in seawater. The chemistry is well understood and has been investigated extensively in connection with the CO₂ Greenhouse issue. Transport models are more complex because currents can carry CO₂ over the entire basin of the South China Sea within a period of months. Data for the three dimensional, time dependent current distribution do not exist. Our models consider diffusion and advection with parameterizations characteristic of expected dynamics. While simplified, the models are readily interpretable, and serve to estimate the order of magnitude of likely transport effects.

Carbon in seawater is not inert, CO₂ rapidly partitions itself into carbonate and bicarbonate species, changing the oceanic pH. If the pH falls below 7.4, calcite in shells begins to dissolve. Increases in carbon become magnified in their effect on the partial pressure of dissolved CO₂. When the partial pressure of CO₂ in the ocean exceeds the partial pressure of CO₂ in the air, CO₂ degasses to the atmosphere. As sparged CO₂ builds up in the basin it will begin to degas. After a time which we refer to as the "retention time" CO₂ will degas at a rate equal to the injection rate from the sparger.

The principal conclusions from our models are that (1) the retention time is only about ten years or less, and (2) addition of CO₂ raises the acidity of seawater sufficiently to cause dissolution of calcite over an area of order 1000 square km in size. These effects indicate that sparging offers no advantage over direct atmospheric venting of CO₂.

At this time, no further work on this project is planned.

Brian P. Flannery, Andrew J. Callegari, Bahlin Nair, and Wayne G. Roberge

1. INTRODUCTION

Initial plans for development of natural gas discovered off Natuna Island in the South China Sea produce as waste gas approximately 65×10^6 metric tons of CO_2 per year (1.5×10^{12} moles CO_2 per year). Release of this amount of CO_2 to the atmosphere raises concern with respect to its effect on the CO_2 greenhouse problem. Global fossil fuel emissions of CO_2 currently amount to about 1.8×10^{10} metric tons per year, so Natuna would represent about 0.4% of world CO_2 emissions, but would occur as a localized point source.

Various descriptions of the Natuna project cite different values for the amount of CO_2 produced. Slight differences arise depending on the assumed production capabilities of the offshore platforms, major differences arise depending on the number of platforms in use. Our figure assumes total production of 5540 million standard cubic feet per day of raw gas from three platforms required to handle the "Pipeline" and "LNG" projects. None of the major conclusions of this report are materially affected by slight changes in the overall production rate.

A possible disposal option that might not lead to atmospheric release of CO_2 involves pumping waste gas back to the sea floor. The idea of using the deep ocean to dispose of industrial CO_2 was proposed by Marchetti (1977). Hoffert et al. (1979) investigated the proposal in more detail and found that injection of CO_2 onto the seafloor at 4000 m depth would prevent CO_2 from entering the atmosphere for a time of order 1000 years. In this study, we investigate the consequences of CO_2 addition to seawater in the shallow basin near the Natuna site. We focus on two principal features (1) the role CO_2 addition on seawater chemistry, especially pH, and (2) the retention time for CO_2 to remain dissolved in seawater before degassing to the atmosphere.

Figure 1 shows geographical features of the site in the South China Sea basin. Over much of the basin the seafloor is not at great depth, but lies on a flat, shallow shelf where the water depth does not exceed 200 m. Monsoons sweep the basin at six month intervals driving and seasonally reversing surface currents that circulate in a gyre over the basin (Wyrki, 1961). We consider discharging CO_2 rich waste gas into seawater near the seafloor through a sparger system as illustrated in Figure 2. The sparger itself consists of a ring approximately 10 km in diameter from which 1.5×10^{12} moles per year of CO_2 would be degassed at a depth of 140 m. Vertically, there are three regions of interest. The sparged CO_2 rises approximately 30 m in a bubble plume before dissolving. At the surface wind and wave action create a well mixed layer of about 30 m depth. Finally, in the middle regions there exists a stably stratified region of about 80 m thickness. Currents near the sparger vary in magnitude and direction with height and time of year. Typical values at depth are of order $10\text{-}50 \text{ cm s}^{-1}$. At the bottom currents are persistently headed southwest, toward Borneo 500 km distant. At the characteristic velocity of 30 cm s^{-1} flow traverses the basin in only 20 days. Thus, advective transport can distribute material injected at Natuna over a basin scale in a time of order months.

Adding CO_2 to seawater decreases the pH and increases the partial pressure $P(\text{CO}_2)$ of dissolved CO_2 . As described in Section 2, the chemistry of CO_2 in seawater is well understood, and has received much attention recently in the context of the role of the oceans as a sink for atmospheric CO_2 in the CO_2 greenhouse problem. At the ocean's surface, gaseous CO_2 is exchanged with the atmosphere whenever a difference exists between the partial pressure of CO_2 in the atmosphere $P_A(\text{CO}_2)$ and the partial pressure of CO_2 dissolved in

surface seawater $P_S(\text{CO}_2)$. CO_2 flows from the reservoir with higher pressure to the reservoir with lower pressure. Thus, CO_2 will degas to the atmosphere when $P_S(\text{CO}_2) > P_A(\text{CO}_2)$.

In Section 3 we define a CO_2 retention time for the Natuna problem according to the concept of time taken for seawater to reach a steady-state concentration of CO_2 . For Natuna that occurs when the ocean has taken up so much CO_2 that it degasses to the atmosphere at the same rate that spargers inject CO_2 at the bottom. Estimates in Section 3 illustrate the central idea of retention time, and establish its order of magnitude for a seawater basin in which CO_2 rapidly mixes throughout the entire volume.

A complete investigation of mixing and transport would require detailed current information in three dimensions and time throughout the South China Sea basin. Such data does not exist, and, even if it did, to use it would require a massive computational simulation. Instead we develop insight and understanding using simplified models and analysis. Nonetheless, these simpler models allow us to estimate the magnitude of the retention time and impact on pH. In Section 4 we consider several classes of models that include the effects of transport by diffusion and advection. Typically, such models predict retention times longer than estimates based on the simple well-mixed model described in 3, but retention time still remains short compared with the timescale of climate change in the CO_2 greenhouse problem. On the other hand, transport models show greater pH reductions near the sparger than the well-mixed model described in Section 3.

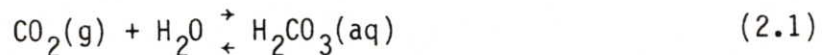
Finally, in Section 5 we discuss these results in the context of the global CO_2 greenhouse problem. Our conclusion is that atmospheric discharge is preferable to seawater sparging. In any event, seawater sparging is nearly

equivalent to atmospheric release since the retention time is short compared with times relevant to the buildup of atmospheric CO₂ influencing climate through a greenhouse effect.

2. CO₂ CHEMISTRY IN SEAWATER

The chemistry of CO₂ in seawater has been discussed at length in many recent references. Our discussion follows that of Takahashi et al. (1980), also see Baes (1982) who developed a graphical representation of the results that is particularly convenient for us. For the Natuna project, the salient features of CO₂ chemistry are the variation in pH and P(CO₂) produced by changes in the total amount of carbon, TC, dissolved in seawater. Changes in pH directly influence chemical reactions, such as the oxidation of H₂S and solubility of calcium carbonate, that influence toxicity. P(CO₂) in surface water controls the direction and rate of gaseous CO₂ exchange between air and sea that determine the length of time that sparged CO₂ will remain in the ocean. The essential result from consideration of CO₂ chemistry is that small increases in TC cause decreases in pH and large increases in P(CO₂).

CO₂ added to seawater rapidly dissolves to form hydrated CO₂ and carbonic acid H₂CO₃. In turn, the carbonic acid can dissociate to form bicarbonate HCO₃⁻ and carbonate CO₃²⁻ ions



where (g) and (aq) denote gaseous and dissolved aqueous CO₂. All reactions proceed rapidly enough that the ultimate distribution of carbon among the three species can be described by equilibrium constants

$$K_1 = [\text{H}_2\text{CO}_3]/P(\text{CO}_2) \quad (2.4)$$

$$K_2 = \text{H}^+[\text{HCO}_3^-]/[\text{H}_2\text{CO}_3] \quad (2.5)$$

$$K_3 = [\text{H}^+][\text{CO}_3^{2-}]/[\text{HCO}_3^-] \quad (2.6)$$

Note that reactions (2.2) and (2.3) depend directly on the oceanic pH. The equilibrium "constants" depend on temperature, pressure, and salinity.

For a given addition of CO₂ to seawater we want to determine the resultant change in pH and the partial pressure P(CO₂). In general, we can predict those quantities given the titration alkalinity TA, the temperature, and the total amount of carbon TC, defined as

$$\text{TC} = [\text{H}_2\text{CO}_3] + [\text{HCO}_3^-] + [\text{CO}_3^{2-}] \quad (2.7)$$

TC measures carbon concentration per unit mass, occasionally we also reference carbon abundance with respect to volume, $tc = \rho\text{TC}$, where the density of seawater is 1.025 gm cm⁻³. At Natuna a typical value for TC is 1930 μmole kg⁻¹ or 1.98 moles m⁻³. Titration alkalinity, a quantity measurable with high precision, represents the net molar concentration of positive ions whose abundance is not sensitive to pH. The excess cationic charge resulting from dissociation of strong electrolytes in seawater is balanced by the anionic charges which are mainly generated by dissociation of carbonic and boric acid. Thus, the titration alkalinity is:

$$TA = [\text{HCO}_3^-] + 2[\text{CO}_3^{2-}] + [\text{H}_2\text{BO}_3^-] + [\text{OH}^-] - [\text{H}^+] \quad (2.8)$$

Effects of other minor species such as silicic and phosphoric acids are neglected. In seawater TA is dominated by dissociated salt species. Consequently, TA is a function of salinity, and does not depend on TC. Given TC, TA, temperature, and functional relations defining the equilibrium coefficients, the set of equations can be solved for consistent values of pH, $P(\text{CO}_2)$, and the abundances of the carbon species. For the equilibrium coefficients we use recent values supplied by Taro Takahashi of Lamont Doherty (Takahashi et al., 1982).

Results for effects of local chemistry are shown in Figure 3-4 which illustrate the dependence of pH and $P(\text{CO}_2)$ on TA and TC for temperatures of 20, and 30°C, representative of surface and deep water near the Natuna drilling site. Based on the global correlation between salinity and TA (Takahashi et al., 1982), Takahashi estimates that TA near Natuna should be about 2300 $\mu\text{eq/kg}$. Air sea exchange tends to maintain equatorial waters nearly in equilibrium with atmospheric $P(\text{CO}_2)$ at a value of 340 μatm . Thus, surface waters at Natuna have a value $\text{TC} = 1930 \mu\text{mol/kg}$ as shown in Figure 3.

The important feature shown in Figures 3-4 is the strong increase in $P(\text{CO}_2)$ and decrease in pH for increases in TC at fixed salinity and temperature which arises from the well known buffer factor in seawater. Notice that increases of only 10% in TC increase $P(\text{CO}_2)$ from 340 μatm to over 1000 μatm and decrease pH from 8.2 to 7.4. In the stippled regions of Figures 3-4 calcium carbonate is undersaturated so that shell material will dissolve, unless biological activity offsets the dissolution rate. The figures illustrate that CO_2 is less soluble at higher temperature. Thus, for a given absolute value TC, pH is lower and $P(\text{CO}_2)$ higher at higher temperature.

That $P(\text{CO}_2)$ increases rapidly with TC is well known (e.g. Weiss, 1974); the ratio of proportional variation for small increments is known as the Revelle factor γ , defined as

$$\Delta P(\text{CO}_2)/P(\text{CO}_2) = \gamma \Delta \text{TC}/\text{TC} \quad (2.9)$$

For surface waters at Natuna we calculate $\gamma = 9.2$. For surface water, the Revelle factor ranges from 8 in warm waters to 15 in cold waters, globally averaging 10 (Broecker et al., 1979; Takahashi et al., 1980). The Revelle factor is especially useful for analysis of the CO_2 retention time as described in the next section.

We can use results of this section to estimate the impact of sparging in the near vicinity of the sparger itself, on length scales of order 10 km when local seawater transport is dominated by advection. We assume that the CO_2 influx, $Q = 1.5 \times 10^{12}$ moles/year, is released uniformly into a seawater flowing over the sparger 10 km wide by 30 m high, the height of the bubble plume (h_B). Then the change in t_c caused by sparging is given by

$$\Delta t_c = \frac{\text{CO}_2 \text{ flow rate}}{\text{water flow rate}} = \frac{Q}{D \cdot h_B \cdot v} \quad (2.10)$$

$$\Delta t_c \text{ (moles m}^{-3}\text{)} = 1.6 \left(\frac{Q}{1.5 \times 10^{12} \text{ moles yr}^{-1}} \right) \left(\frac{10 \text{ km}}{D} \right) \left(\frac{30 \text{ m}}{h_B} \right) \left(\frac{10 \text{ cms}^{-1}}{v} \right)$$

Figure 5 shows t_c vs. velocity in the range 1-100 cm s^{-1} , and the corresponding variation in local $P(\text{CO}_2)$ and pH. Note that if local stagnation events occur they will be accompanied by large changes in local pH. Onsite measurements indicate that velocities less than 10 cm s^{-1} do occur occasionally.

3. THE SEA-AIR EXCHANGE OF CO₂ AND THE CO₂ RETENTION TIME

Gaseous CO₂ migrates across the sea air surface interface at a net rate F_{SA} proportional to the difference between the partial pressures of CO₂ in the two reservoirs

$$F_{SA} = E \left[\frac{P_s(\text{CO}_2) - P_A(\text{CO}_2)}{340 \mu\text{atm}} \right] \quad (3.1)$$

The expression has been scaled to units appropriate for the annual mean yearly average partial pressure of atmospheric CO₂, P_A(CO₂) = 340 μatm. Empirical calibrations give E = 20 moles/(m² yr) (Peng et al. 1979). For surface conditions at Natuna, t_{c_{eq}} ≈ 2.0 moles m⁻³ is required for P_S(CO₂) = 340 μatm, at which F_{SA} vanishes. Surface waters over most of the worlds oceans maintain a carbon abundance such that F_{SA} ≈ 0.

To estimate the appropriate timescale, t_{eq}, for air-sea gas exchange to equilibrate, consider a situation in which a well-mixed layer of seawater of depth h contains no CO₂ initially, and is in contact with air at P_A(CO₂) = 340 μatm. For typical oceanic conditions the well-mixed layer has a depth h = 75 meters. To reach equilibrium the mixed layer requires the addition of h·t_c = 140 moles m⁻², and the initial filling rate is 20 moles/(m² yr). Thus, a characteristic estimate for the equilibration time scale is

$$t_{eq} = \frac{h t_{c_{eq}}}{F_{SA}} \approx 7 \text{ yr} \quad (3.2)$$

After time of order t_{eq} the net exchange of CO₂ between air and sea vanishes and t_c reaches steady state in the ocean.

While the estimate for air sea exchange equilibration time in (3.2) considered no additional sources, for the Natuna problem the CO_2 concentration in seawater will not reach equilibrium until the ocean waters lose CO_2 at a rate identical to the influx from the sparger Q . In later sections we will consider more detailed models including diffusion and transport, our goal here is to obtain simple estimates for the characteristic timescale of the problem. We estimate the retention time τ_R for CO_2 by first estimating what the carbon concentration $t_{c_{\text{eq}}}$ in surface waters must be in order for surface outflux to equal Q . We then estimate the equilibration time assuming by that the necessary increase in t_c occurs at a rate Q .

Nothing in the estimates used here actually allows us to determine the basin size, or surface area over which degassing occurs, we will attempt to estimate basin size in later sections. Here we solve for retention time as a function of assumed surface area for a circular region of arbitrary radius R . Because the carbon chemistry of seawater produces such a strong increase in $P(\text{CO}_2)$ with increase in total CO_2 the retention time is very short for small basin sizes. For large basin size, the retention time approaches a limiting value that does not depend on radius. Thus, we will obtain useful (lower) bounds on the retention time even without knowing the size of the affected region.

For a circular surface area of radius R the net outflux of CO_2 from sea to air will equal the sparger influx for

$$\pi R^2 F_{\text{SA}} = Q \tag{3.3}$$

$$\frac{\Delta P(\text{CO}_2)}{340 \text{ } \mu\text{atm}} = 2.4 \left[\frac{Q}{1.5 \times 10^{12} \text{ moles yr}^{-1}} \right] \frac{100 \text{ km}^2}{R}$$

To estimate the increase in TC required to produce the change $\Delta P(\text{CO}_2)$ we must solve the non-linear chemistry equations of the previous section. However, for small changes in TC we can use the Revelle factor to determine the concentration change directly.

$$\pi R^2 E \gamma \left(\frac{\Delta \text{TC}}{\text{TC}} \right) = Q \quad \text{for} \quad \frac{\Delta \text{TC}}{\text{TC}} \ll 1 \quad (3.4)$$

$$\frac{\Delta \text{tc}}{\text{tc}} = 0.26 \left[\frac{Q}{1.5 \times 10^{12} \text{ mole yr}^{-1}} \right] \left[\frac{100 \text{ km}^2}{R} \right]$$

Note that initially $P_S(\text{CO}_2) = P_A(\text{CO}_2) = 340 \mu\text{atm}$, and that $\Delta \text{tc}/\text{tc} = \Delta \text{TC}/\text{TC}$.

Given the increase in TC, either from (3.4) or by solution of the nonlinear equation (3.3) we can crudely estimate the time for the ocean to reach equilibrium as in the discussion for t_{eq} in (3.2). Assume that the entire basin of volume $\pi R^2 h$ must increase its CO_2 concentration by Δtc , and use the initial influx rate Q to estimate the filling time

$$\tau_R = \frac{\pi R^2 h \Delta \text{tc}}{Q} \quad (3.5)$$

For the Natuna basin we use $h = 140 \text{ m}$. If the required change Δtc is small, then we can use (3.4), based on the Revelle factor, to determine τ_R .

$$\tau_R = \frac{h \text{ tc}}{\gamma E} \approx 1.4 \text{ yr} \quad \text{for} \quad \frac{\Delta \text{tc}}{\text{tc}} \ll 1 \quad (3.6)$$

Notice that this estimate is independent of the basin size R and the influx rate Q .

The crude estimate derived here represents an approximation corresponding to adding CO_2 to the entire cylindrical volume of the basin as though the concentration remained well mixed at all times. This is unlikely to occur both because the water is stably stratified vertically and because advective transport controls horizontal distribution. In later sections we consider such additional effects. Nonetheless, these estimates place the characteristic timescale in perspective, it is of order years.

Using these estimates, and accurate solution of the nonlinear equation (3.3) to determine t_c appropriate to equilibrium degassing for $P(\text{CO}_2)$, we illustrate several features of the results in Figure 6. In Figure 6a and b we show the required change in $P(\text{CO}_2)$ and t_c as a function of basin size. Figure 6c shows the retention time estimated from (3.5). Given the increase in t_c we also show the pH corresponding to equilibrium conditions. The important point is that, if rapid mixing occurs on small length scales, of order of sparger diameter, 10 km, then the degassing time is very short regardless of the exact size of the affected region. Over larger scales the degassing time will still be only a few years if CO_2 reaches the surface.

Detailed models of transport phenomenon as discussed below increase these time estimates.

4. TRANSPORT MODELS

Injected CO_2 from the sparger dissolves into seawater in a bubble plume within 30 m of the seafloor. Measurements of vertical profiles of temperature and density at the site indicate that below a well-mixed surface layer 30 m deep the water is stably stratified, so vertical mixing must proceed by eddy diffusion, sporadic upwelling events, or complex non-local transport by currents. Our estimates below will show that vertical diffusion

times of order a few years are required to bring CO_2 to the surface. As described in the introduction, measured horizontal velocities of order 30 cm s^{-1} carry material over basin scale distances in only months. Site measurements also indicate that current varies significantly with depth and time. Consequently, a realistic model of seawater transport of CO_2 in the South China Sea requires current information covering the entire basin in three spatial dimensions and time.

To date no complete data set exists to carry out a realistic transport calculation on the scale of the basin, and such a calculation presents a formidable numerical exercise even if the data were available. To gain insight into the likely retention time for CO_2 we investigate a hierarchy of simpler models based on assumed current and diffusion profiles, that do include time dependence. Cumulatively, they indicate that CO_2 retention times will be of order a decade at most, barring unlikely current patterns, or anomalously low vertical diffusion rates, as we describe.

The models described below have analytical solutions for the time dependent variation of concentration when F_{SA} can be approximated by a linear dependence on concentration, using the Revelle factor in (3.1). However, numerical solutions are simple to obtain, even with non-linear relations for the loss term, and simple to interpret based on known characteristic behavior for the diffusion equation. Table 1 contains a listing of model parameters and typical values for their magnitude.

$K(V)$ and $K(H)$ representing vertical and horizontal diffusion in the ocean are the only parameters listed in Table 1 that have not yet been discussed. Below the mixed layer of the ocean, variation of temperature and density produce stable stratification that inhibits vertical flow of any sort, including diffusive mixing. $K(V)$ is particularly important in this problem

since it sets the timescale for carbon to diffuse to the surface where losses can occur by air-sea exchange. The value we list, $4000 \text{ m}^2 \text{ yr}^{-1}$ ($= 1.3 \text{ cm}^2 \text{ s}^{-1}$) is typical of vertical diffusion through stably stratified layers in the ocean as a whole (Broecker and Peng, 1982). A recent study of Berelson et al. (1982), based on the vertical distribution of radon-222 in the Santa Barbara basin of the California coast, found $K(V) = 4 \text{ cm}^2 \text{ s}^{-1}$ at water depths of 500 m. No measurements of $K(V)$ exist for the Natuna basin.

It is possible that wave action and currents in a confined basin make $K(V)$ become larger, reducing the upward diffusion time, or that special circumstances cause $K(V)$ to be smaller than for the ocean as a whole. No a priori theory exists that can accurately predict values for $K(V)$.

Horizontal diffusion is known to be dramatically larger than vertical, $K(H) = 10^7 K(V)$, is generally accepted (Kuo and Veronis, 1973; Sarmiento et al., 1982). However, the model results are less sensitive to $K(H)$, since advective current flow tends to dominate diffusion as a cause for horizontal mixing.

a. Models With Rapid Horizontal Mixing and Vertical Diffusion

In the previous section we estimated the retention time of a well-mixed cylindrical model based on the required equilibrium concentration and initial influx rate. Here we consider the time history of such a model, and add effects due to vertical diffusion. Since surface losses rise as CO_2 increases in the reservoir, the actual history of outgassing causes the retention time to increase over that estimated in the previous section.

In this model we assume that horizontal mixing throughout the basin of radius R occurs rapidly at any depth, but that vertical transport occurs only by diffusion in the stratified layers below the surface mixed layer of depth h_M . The CO_2 injection rate per unit volume $q(z)$ is taken to be uniform per unit volume at depths within the bubble plume, $z < h_B = 30$ m. The equation defining the time history of concentration is

$$\frac{\partial tc}{\partial t} = q(z) + \frac{\partial}{\partial z} K(V) \frac{\partial tc}{\partial z} \quad (4.1)$$

where

$$q(z) = \frac{Q}{\pi R^2 h_B} \quad \text{for } z < h_B$$

$$q(z) = 0 \quad \text{for } z > h_B$$

Here z represents height above the seafloor in a water column of total depth H . Boundary conditions for (4.1) correspond to separate treatment of the CO_2 balance in the mixed layer and zero diffusive flux across the seafloor.

$$\frac{\partial tc(M)}{\partial t} = - K(V) \frac{\partial tc}{\partial z} \Big|_{H-h_M} - \frac{F_{SA}}{h_M} \quad (4.2a)$$

$$\frac{\partial tc}{\partial z} \Big|_{z=0} = 0 \quad (4.2b)$$

Several features of the model should be noted. First, from the form of (4.1-2) the solution depends only on the basin area πR^2 , and volume $\pi R^2 H$, but not on the assumed cylindrical geometry; we use R simply as a convenient

measure of basin size. Second, in the limit where $K(V)$ becomes very large this model becomes vertically (and horizontally) well mixed, as in the simpler model of Section 3. Mathematically, the vertically well mixed model corresponds to just using the boundary conditions (4.2a) and letting the mixed layer depth equal H . Third, just as in Section 3, these equations reach equilibrium when surface degassing balances sparger injection. Therefore, equilibrium requires the same value for surface concentration as found in (3.3). However, with vertical diffusion t_c increases with depth; thus, for a given value of t_c at the surface, the reservoir has a higher capacity for CO_2 . The retention time increases from the estimate in Section 3, both because some degassing occurs as the CO_2 concentration rises and because the basin capacity increases.

We illustrate the character of the time dependent solutions in Figure 7 which shows the rate of surface degassing relative to the sparger injection rate for a series of models with basin size 500 km. The three curves are for (1) a vertically well-mixed model, (2) $K(V) = 4000 \text{ m}^2 \text{ yr}^{-1}$ which is the most reasonable estimate for the diffusion coefficient, and (3) a model with $K(V) = 400 \text{ m}^2 \text{ yr}^{-1}$, an order of magnitude lower than the diffusion coefficient typical of the global ocean. These models all display an initial phase where the degassing rate increases relatively rapidly as CO_2 begins to fill the basin, followed later by a slow relaxation to steady state where degassing would equal the influx from the sparger.

While the model takes infinite time to reach the exact steady state, we can assign a nominal retention time, τ_R , based on the condition that CO_2 degassing equals some large fraction of the injection rate, say 90%. Figure 8 shows the retention time estimated in that way for a series of models with varying radius and diffusivity. Note that vertical diffusion increases the

retention time relative to well mixed models, as discussed above, but for our best estimate of $K(V)$, the retention time is still only about 3.5 years even for the largest basin size.

Figure 9 shows the variation with depth of CO_2 concentration t_c and pH for models in steady state. In steady state the flux of CO_2 is constant with depth so $K(V)dt_c/dz = F_{SA}$. Thus the CO_2 concentration profiles are nearly linear with depth. (The relation becomes curved inside the bubble plume where the source function varies with depth.) Notice that models with longer retention time also have higher concentrations of CO_2 at the seafloor.

Finally, we use this model to illustrate sensitivity of retention time to sparger depth. Figure 10 shows a series of models with $K(V) = 4000 \text{ m}^2 \text{ yr}^{-1}$, our best estimate, and a range of values for H , the sparger depth. In each case, we include a bubble plume of 30 m and a mixed layer of 30 m, but we vary the depth H from 60 to 1000 m. The results follow the basic scaling appropriate to propagation of a diffusion front over a distance L

$$L^2 \propto Kt \quad (4.3)$$

Thus, retention times become dramatically longer as the sparger depth increases.

Our results showing very long retention times for disposal at great depth are in agreement with those of Hoffert et al. (1979) who investigated disposal in the deep ocean at 4000 m. If currents along the bottom of the South China Sea basin fortuitously carried CO_2 from the Natuna site to deep water, then retention times would be increased. An area of deep water (>1000 m) does exist a few hundred kilometers to the northeast. Although currents could carry CO_2 over such distances, buoyancy effects are likely to prevent currents from penetrating to great depth.

b. Rectangular Models With Horizontal Advection and Vertical Diffusion

Models in Section (4a) were shown for a series of basin sizes, but nothing in the physical description established the basin size. In nature the interplay between horizontal and vertical transport establishes a scale: CO₂ is not lost until it encounters the surface but, during the time taken to rise, CO₂ also migrates horizontally. For the Natuna site there is no question that significant horizontal motion occurs, the problem is that time and velocity scales are sufficiently long that basin scale circulation must be included to evaluate the spreading. With a typical velocity of 30 cm s⁻¹ directed southeast at depth, CO₂ injected at the Natuna site reaches the coast of Borneo, 500 km distant, in only 20 days, which is short compared with the retention time (unless rapid vertical mixing occurs). If the current persists that far, then at Borneo the direction will deflect along the coast, and enter into circulation on a basin scale size, for which three dimensional time dependent data do not exist.

Bearing in mind the preceding discussion, we consider two dimensional advective, diffusive flow merely to establish the general character of the solution, rather than to model basin scale circulation. We consider uniform advection with velocity v along the x direction, in a rectangular basin of width W , transverse to the flow. W is not determined by the model. We assume that CO₂ mixes rapidly along the width, and that the CO₂ source is distributed smoothly along a 10 km section in x of width W . The model is defined by the following equations and boundary conditions

$$\frac{\partial tc}{\partial t} = \frac{\partial}{\partial z} K(V) \frac{\partial tc}{\partial z} - \frac{\partial (v \cdot tc)}{\partial x} + q(x,z) \quad (4.4)$$

$$\frac{\partial tc(M)}{\partial t} = -K(V) \frac{\partial tc}{\partial z} \Big|_{H-h_M} - \frac{\partial [v \cdot tc(M)]}{\partial x} - \frac{F_{SA}}{h_M} \quad (4.5a)$$

$$\frac{\partial tc}{\partial z} = 0 \quad \text{at} \quad z = 0 \quad (4.5b)$$

$$\frac{\partial tc}{\partial x} = 0 \quad \text{at} \quad x = x_1 \quad (4.6a)$$

$$\frac{\partial tc}{\partial x} = 0 \quad \text{at} \quad x = x_2 \quad (4.6b)$$

where x_1 , x_2 denote the endpoints of the rectangular model. The boundary conditions in (4.6a,b) apply at the "x" boundaries of the rectangle. These conditions imply that there will be zero diffusive flux through the boundaries. This is a good approximation since advection dominates the flow.

We consider two models of the advective diffusive class, both have width $W = 10$ km, with a sparger source distributed along 10 km length in x . The first model is well mixed vertically ($K(V) \rightarrow \infty$), the second has $K(V) = 4000 \text{ m}^2 \text{ yr}^{-1}$. Figure 11 illustrates the variation of concentration with distance for the well mixed model. Here the total length of the model is 10^4 km, with the sparger source centered at $x = 505$ km. Because the model is well mixed, degassing commences directly over the sparger, and the concentration decays with distance downstream from the sparger. The advective timescale, $(x_2 - x_1)/v = 1$ yr, controls approach to steady state in this model, so that concentration achieves steady state values as the flow front passes a given point. At this relatively high rate of flow, even within 10^4 km of the sparger, the net rate of surface degassing only reaches about 50 percent of the sparger injection rate. Further degassing of CO_2 would occur beyond x_2 , the downstream limit of our computational domain. However, we terminated the calculation at 10^4 km because the geometrical distance greatly exceeds the size of the South China Sea basin.

The second advective diffusive model resembles the first, but includes vertical diffusion with $K(V) = 4000 \text{ m}^2 \text{ yr}^{-1}$ rather than being well mixed. The basin length in this model is only 10^3 km , with the sparger located at 95 km. For this model both the advective and diffusive times play a role in the approach to steady state. Here advected flow crosses the grid horizontally in a time $(x_2 - x_1)/v = 0.1 \text{ year}$, but the vertical diffusion time, $H^2/K(V) = 3 \text{ years}$, is much longer. Figure 12 illustrates the time dependent solution for the total rate of surface outgassing over the entire grid. Net outflow only approaches steady state after 3 years, the diffusive timescale. At that time, the surface outgassing rate is 35 percent of the injection rate. Again, as in the previous model, further degassing would occur beyond the downstream boundary at x_2 . Figure 13 shows contours of constant pH for this model after the flow achieves equilibrium. Notice that pH indicates large increases in acidity near the sparger.

The essential point to be learned from the advective diffusive models discussed here is that the vertical diffusion time is sufficiently long that advection can transport CO_2 over distances large compared with the basin size of the South China Sea. It is unrealistic to assume that such flow would remain confined to a geometry resembling flow in a basin of rather narrow rectangular cross section as assumed here, i.e. with W constant. It follows that current behavior far from the Natuna site might control the ultimate fate of CO_2 . For instance, it is possible that currents flowing at depth near the site, might upwell as they approach the coast of Borneo, so that outgassing occurs at that point. On the other hand, currents could carry CO_2 to deep water increasing the retention time.

One other point learned from this model is that, when advection dominates the flow, the local concentration in the vicinity of the sparger is

governed by the considerations described in Section 2. There we analyzed for peak local concentration simply by constructing the ratio of the CO₂ injection rate to the water flow rate. The important point from that analysis was that CO₂ concentrations become very large, and pH is strongly reduced, during periods when the flow velocity stagnates over the sparger.

c. Axisymmetric Models With Radial and Vertical Diffusion

Guided by insight from the previous models we consider one final model in which diffusion occurs in both the vertical and radial dimensions, but without advection. The motivation for this model is an attempt to approximate the effect of variable horizontal currents on transport as a diffusion process. Our estimate for the horizontal diffusion coefficient K(H) obtained in this fashion, agrees approximately with oceanographic estimates for K(H) suitable for open ocean conditions. Such estimates show that the ratio K(H)/K(V) is of order 10⁷ or more (Kuo and Veronis, 1973; Sarmiento, 1982). The enormous enhancement occurs because horizontal dynamical processes are not damped by stratification, as in vertical diffusion.

We estimate the horizontal eddy diffusivity for random horizontal current patterns in which the velocity persists at a given value for a specific length of time Δt , and then changes its direction completely. For such a model, the Fickian diffusion coefficient is the average value of the product of length and velocity $\langle Lv \rangle$. To estimate a characteristic value for K(H) we use $v = 30 \text{ cm s}^{-1}$, and a persistence time of one day

$$K(H) = \langle Lv \rangle \approx v^2 \Delta t$$

$$K(H) \approx 2.5 \times 10^{11} \text{ m}^2 \text{ yr}^{-1} \left(\frac{v}{30 \text{ cm s}^{-1}} \right)^2 \left(\frac{\Delta t}{\text{day}} \right) \quad (4.7)$$

We stress that we do not know the actual values of $K(H)$ or $K(V)$ at the Natuna site. Our estimate for $K(H)$ is solely for motivational purposes. It does, however, agree roughly with estimates characterizing the open ocean.

In the model below we use $K(H)/K(V) = 5 \times 10^7$. For this ratio, and a typical basin size, diffusive transport over the vertical distance, 100 m, occurs in times comparable with transport horizontally over 500 km. This follows from (4.3) since $(R/H)^2[K(V)/K(H)] = 0.5$

With this picture for diffusion we can model the basin as an axisymmetric two dimensional diffusion problem:

$$\frac{\partial tc}{\partial t} = q(r,z) + \frac{1}{r} \frac{\partial}{\partial r} K(H) r \frac{\partial}{\partial r} tc + \frac{\partial}{\partial z} K(V) \frac{\partial tc}{\partial z} \quad (4.8)$$

$$\frac{\partial tc(M)}{\partial t} = \frac{1}{r} \frac{\partial}{\partial r} K(H) \frac{\partial}{\partial r} tc - \frac{K(V)}{h_M} \frac{\partial tc}{\partial z} \Big|_{H-h_M} - \frac{F_{SA}}{h_M} \quad (4.9a)$$

$$\frac{\partial tc}{\partial z} \Big|_{z=0} = 0 \quad (4.9b)$$

$$\frac{\partial tc}{\partial r} \Big|_{r=0} = 0 \quad (4.10a)$$

$$\frac{\partial tc}{\partial r} \Big|_{r=R} = 0 \quad (4.10b)$$

Figure 14 shows that the time dependent variation of outgassing for a single model with a radius of 500 km, typical of the basin size. The model reaches 90% outgassing in 6.5 years.

Without detailed data and simulations of three dimensional time dependent CO_2 transport, the model described here represents our most realistic simulation of the CO_2 retention time. From previous models it is clear that, for typical values of vertical diffusivity, CO_2 will mix to the surface

in a timescale of a few years, after which outgassing to the atmosphere will match CO₂ injection rates. Also, the models, and simple physical estimates, show that a timescale of a few years allows transport to distribute CO₂ throughout the South China Sea basin.

5. SUMMARY

Because of concern about the CO₂ greenhouse issue, seawater sparging of waste gas CO₂ from the Natuna project was proposed as an alternative to direct atmospheric release. However, our results indicate that sparged CO₂ reaches the surface and degasses to the atmosphere within a period less than a decade, which is short compared with the 100 year period projected for CO₂ doubling. Furthermore, increasing the concentration of CO₂ in seawater increases acidity.

For our best estimates of transport properties, vertical diffusion from 140 m depth to surface only requires 6.5 years before the rate of CO₂ outgassing through the sea surface nearly equals the sparger injection rate. Those estimates are based on parameter values determined from studies of the global ocean, conditions could be different in the shallow basin of the South China Sea. If more rapid vertical mixing occurs, the outgassing occurs even faster. Possibly, current patterns might transport CO₂ below the surface for rather large distances, and then upwell in localized regions, perhaps near coastlines. Once CO₂ contacts the surface at high concentration rapid degassing would occur. Alternatively, it is possible that currents could carry CO₂ to deeper water giving a longer retention time, but buoyancy effects probably prevent currents from flowing to great depth.

For typical diffusion rates, the only way to keep CO_2 from degassing quickly is to sparge at far greater depths. Below 1000 km the CO_2 retention time exceeds 100 years. A region of much deeper water is available several hundred km to the northeast, but sparging there would be far more costly since a pipeline would be required, and waste gas must be pumped to greater depth and pressure.

CO_2 in seawater is not inert; increasing the concentration of CO_2 decreases pH (increases acidity). Present ambient conditions have pH = 8.3 in our models. Reduction of 0.7 units to 7.6 pH allows calcium carbonate in the aragonite form to begin to dissolve. Our models indicate that pH reductions of one unit or more will affect regions of order 1000 km^2 . A tradeoff occurs: if the vertical diffusion coefficient decreases, so that CO_2 is retained longer, then the concentration of CO_2 at depth rises. Consequently, when the retention time increases, the impact associated with pH change also increases. Either the size of the affected region grows or the magnitude of the pH change increases, or both.

We also estimated the peak local concentration of CO_2 and associated change in pH, based on advection dominated flow in the vicinity of the sparger, where concentration changes maximize. Those estimates show appreciable pH changes whenever flow speed falls below 50 cm s^{-1} , which occurs commonly. Furthermore, changes rise dramatically during stagnation events when flow speed drops below 10 cm s^{-1} which do occur occasionally.

Our conclusion is that sparging of CO_2 offers little advantage over direct atmospheric release of CO_2 , since the retention times is short in any case, but that sparging of large amounts of CO_2 does cause a negative impact in seawater by its affect on pH.

REFERENCES

- Baes, C. F. (1982), "Effects of Ocean Chemistry and Biology on Atmospheric Carbon Dioxide," 187-204, in "Carbon Dioxide Review: 1982," W. C. Clark editor, Oxford University Press: New York, 1982.
- Berelson, W. M., Hammond, D. E. and Fuller, C. (1982), Radon-222 as a tracer for mixing in the water column and benthic exchange in the southern California borderland, *Earth and Planetary Sciences Letters*, 61, 41-45.
- Broecker, W. S. and Peng, T. H. (1982), "Tracers in the Sea," ELDIGIO Press, Palisades, New York, 690 pp.
- Broecker, W. S., Takahashi, T., Simpson, H. J. and Peng, T. H. (1979), Fate of fossil fuel carbon dioxide and the global carbon budget, *Science*, 206, 409-418.
- Hoeffert, M. I., Wey, Y. C., Callegari, A. J., and Broecker, W. S. (1979), Atmospheric response of deep sea injections of fossil-fuel carbon dioxide, *Climate Change*, 2, 53-68.
- Kuo, H. H. and Veronis, G. (1973), The use of oxygen as a test for an abyssal circulation model, *Deep-Sea Res.*, 20, 871-878.
- Marchetti, C. (1977) on geoengineering the CO₂ problem, *climate change*, 1, 59-68.

- Pens, T. H., Broecker, W. S., Mathieu, G. G. and Li, Y. H. (1979), Radon Evasion rates in the Atlantic and Pacific Oceans as determined during the GEOSECS Program, Jour. Geophys. Res., 84, 2471-2486.
- Sarmiento, J. L., Rooth, C. G. H., and Broecker, W. S. (1982), Radium-228 as a tracer of basin wide processes in the abyssal ocean, Jour. Geophys. Res., 87, 9694-9698.
- Takahashi, T., Broecker, W. S., Werner, S. R. and Bainbridge, A. E. (1980), Carbonate chemistry of the surface waters of the world oceans, in "Isotope Marine Chemistry," E. D. Goldberg, Y. Horibe and K. Saruhashi editors, Uchida Rokakuho Pub., Japan, 291-326.
- Takahashi, T., Williams, R. T. and Bos, D. L. (1982), Carbonate chemistry, in "GEOSECS Pacific Expedition, Vol. 3, Hydrographic Data, 1973-1974, National Science Foundation, Washington, D.C. 78-82.
- Weiss, R. F. (1974), Carbon dioxide in water and seawater: The solubility of a non-ideal gas, Marine Chem., 2, 203-215.
- Wyrtki, K. (1961), NAGA Report, Scientific Results of Marine Investigations of the South China Sea and the Gulf of Thailand, 1951-61, Physical Oceanography of the Southeast Asian Waters, Univ. Calif. Scripps Instit. of Oceanography La Jolla, California, Vol. 2, 195 pp.

TABLE 1

MODEL PARAMETERS

<u>Symbol</u>	<u>Identification</u>	<u>Typical or Starting Value</u>
Q	Total CO ₂ source	1.5 x 10 ¹² moles yr ⁻¹
ρ	Seawater density	1.025 gm cm ⁻³
TC	Total CO ₂ concentration (mass)	1930 μmoles kg ⁻¹
tc = ρTC	Total CO ₂ concentration (volume)	1.98 moles m ⁻³
R	Basin radius	10-1000 km
H	Basin depth	130 m
h _B	Height of bubble plume	30 m
h _M	Depth of surface mixed layer	30 m
F _{SA}	CO ₂ flux from sea to air	moles/(m ² yr)
	$F_{SA} = E[P_S(CO_2) - P_A(CO_2)]/340 \mu\text{atm}$	
E	Exchange coefficient for F _{SA}	20 moles/(m ² yr)
K(V)	Vertical diffusion coefficient	4000 m ² yr ⁻¹
K(H)	Horizontal diffusion coefficient	2 x 10 ¹¹ m ² yr ⁻¹
v	Horizontal current speed	0.30 m s ⁻¹

FIGURE CAPTIONS

FIGURE 1. Geography of the Natuna site.

FIGURE 2. Schematic of the sparger configuration.

FIGURE 3. Variation of $P(\text{CO}_2)$ and pH as a function of alkalinity TA and total carbon tc (per unit volume) at a salinity of 35 o/oo and temperature 20°C corresponding to bottom water at the Natuna site. Calcium carbonate is unsaturated and dissolves when $\text{pH} \lesssim 7.4$.

FIGURE 4. As in Figure 3, but for 30°C corresponding to surface water at the Natuna site.

FIGURE 5. Variation of local total carbon abundance tc (a), $P(\text{CO}_2)$ (b), and pH (c) with current, for flushing at a uniform flow rate over the 10 km sparger diameter. CO_2 is injected at a rate of 1.5×10^{12} moles per year uniformly over the bubble column of height 30 m.

FIGURE 6. Variation of carbon abundance TC (a), $P(\text{CO}_2)$ (b), retention time τ (c), and pH (d) as a function of basin diameter R such that a well mixed reservoir achieves steady state CO_2 concentration. For each model CO_2 degasses to the atmosphere at the same rate as the sparger injects CO_2 .

FIGURE 7. CO_2 surface degassing rate versus time for a horizontally well mixed cylindrical model with radius 500 km. The degassing rate is scaled relative to the CO_2 injection rate from the subsurface sparger. The top curve is for a vertically well mixed model. The middle curve is for our best estimate of the vertical diffusivity. The bottom curve is for diffusivity a factor of ten below our best estimate.

FIGURE 8. Retention time as a function of basin size and diffusivity for the cylindrical model with vertical diffusion and rapid horizontal mixing. The retention time is defined as the time when surface degassing of CO_2 reaches 90% of the sparger injection rate.

FIGURE 9. Variation of (a) CO_2 concentration and (b) pH with height above seafloor for models with varying basin size and diffusivity. These models have reached steady state. With diffusion the concentration varies linearly with depth except in the mixed layer, where concentration is constant, and inside the bubble plume layer where the source function varies.

FIGURE 10. CO_2 surface degassing rate versus time as a function of variable sparger depth, H . As in Figure 7 the degassing rate is scaled relative to the sparger injection rate, and the model is cylindrical with rapid horizontal mixing and vertical diffusion. For all curves $K(V) = 4000 \text{ m}^2 \text{ yr}^{-1}$. The results show that retention time increases roughly as H^2 for fixed diffusivity.

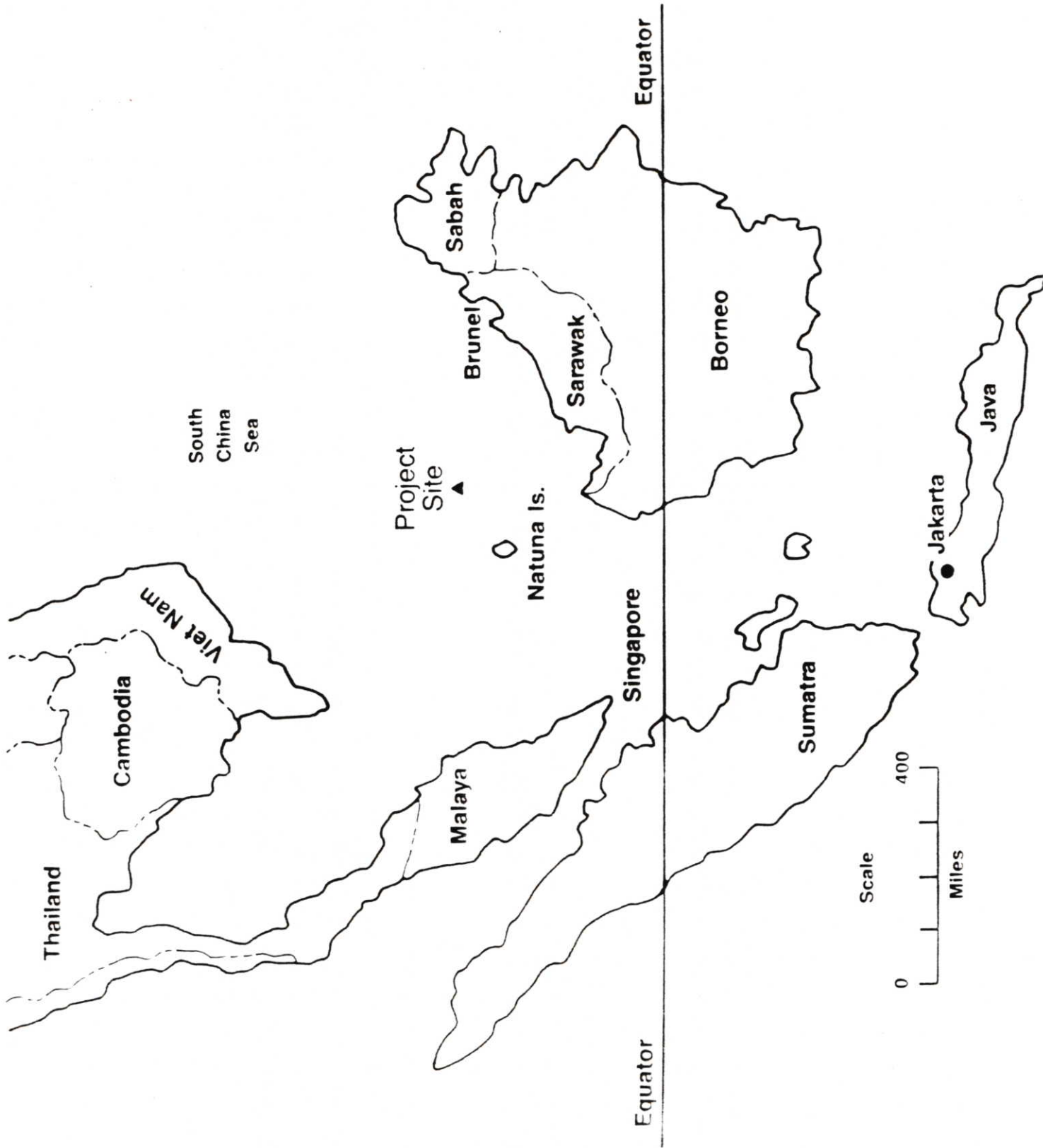
FIGURE 11. Time dependent solution for a well mixed model with advective velocity 30 cm s^{-1} and width 10 km: (a) carbon concentration, (b) surface flux F_{SA} , (c) total surface CO_2 outgassing relative to sparger injection. The 10 km long sparger source is centered at 505 km.

FIGURE 12. Variation of the surface degassing rate with time for a two dimensional advective, diffusive model. The model is 1000 km long by 10 km wide and 140 m high, with the sparger source centered at 95 km. The horizontal advection velocity is 30 cm s^{-1} , and the vertical diffusivity $K(V) = 4000 \text{ m}^2 \text{ yr}^{-1}$. After 3 years the degassing rate within 900 km of the sparger equals approximately 35 percent of the injection rate.

FIGURE 13. Contours of pH for the advective diffusive model shown in Figure 12, after attaining steady state.

FIGURE 14. Variation of the surface degassing rate with time for an axisymmetric model with both vertical and horizontal diffusion. In this model $K(V) = 4000 \text{ m}^2 \text{ yr}^{-1}$, $K(H)/K(V) = 5 \times 10^7$, $H = 140 \text{ m}$, and the basin radius is 500 km.

Figure 1



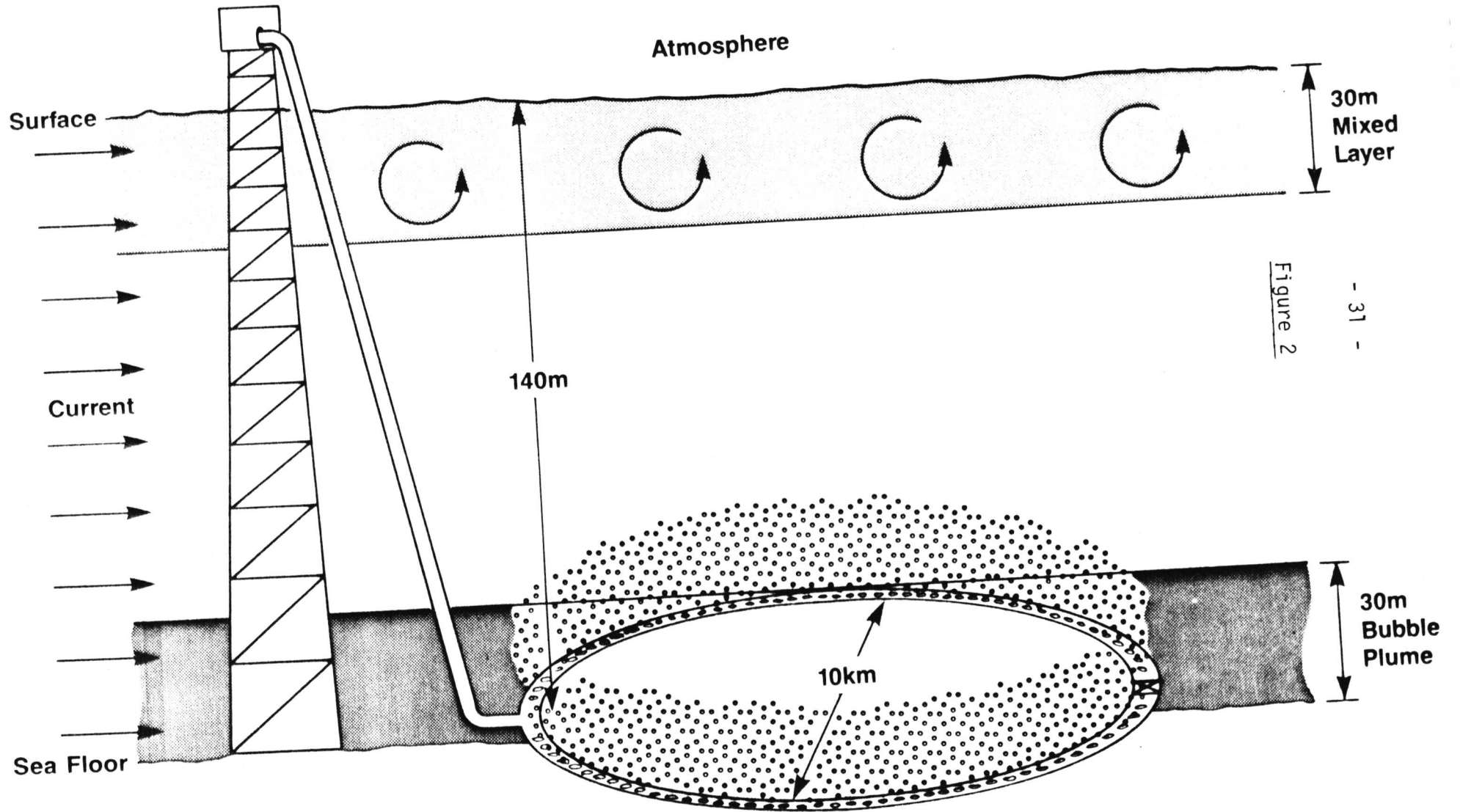


Figure 3

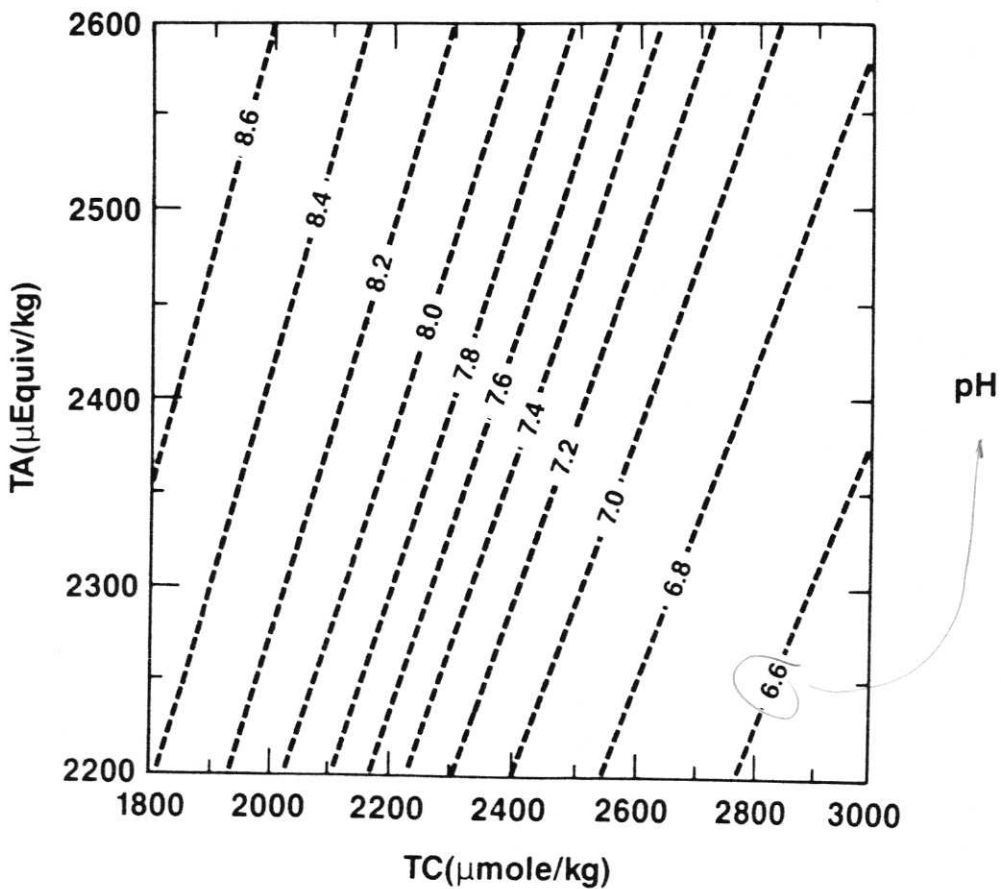
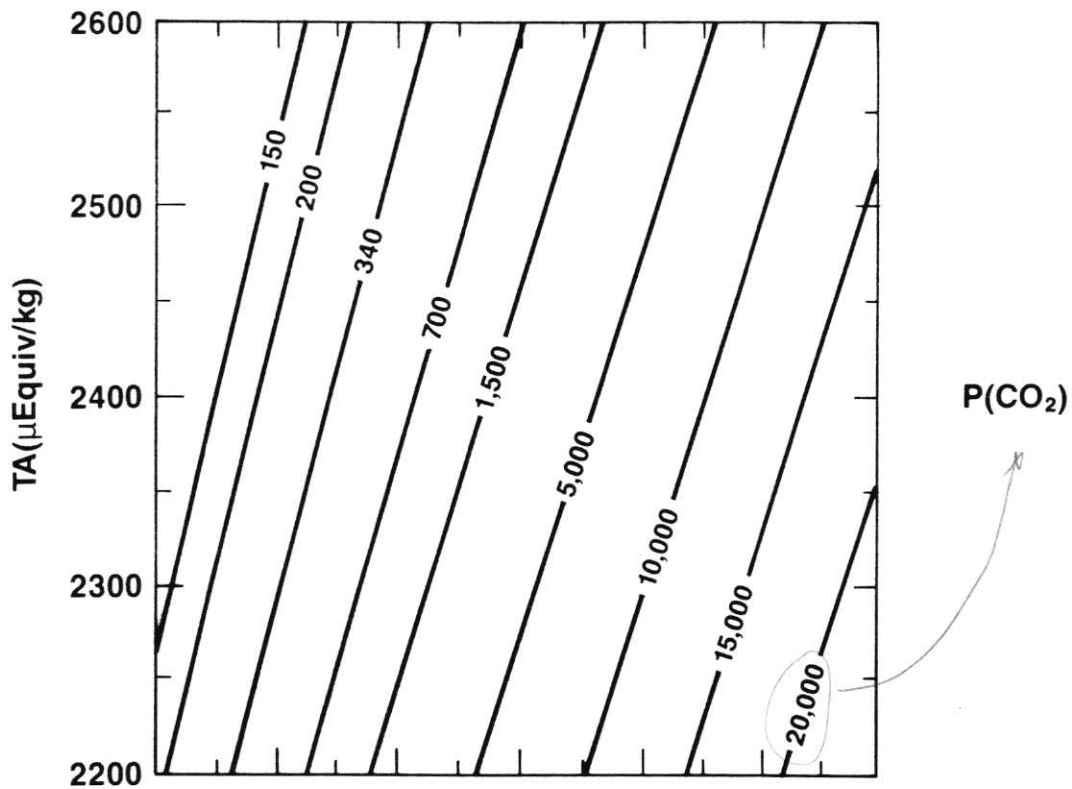


Figure 4

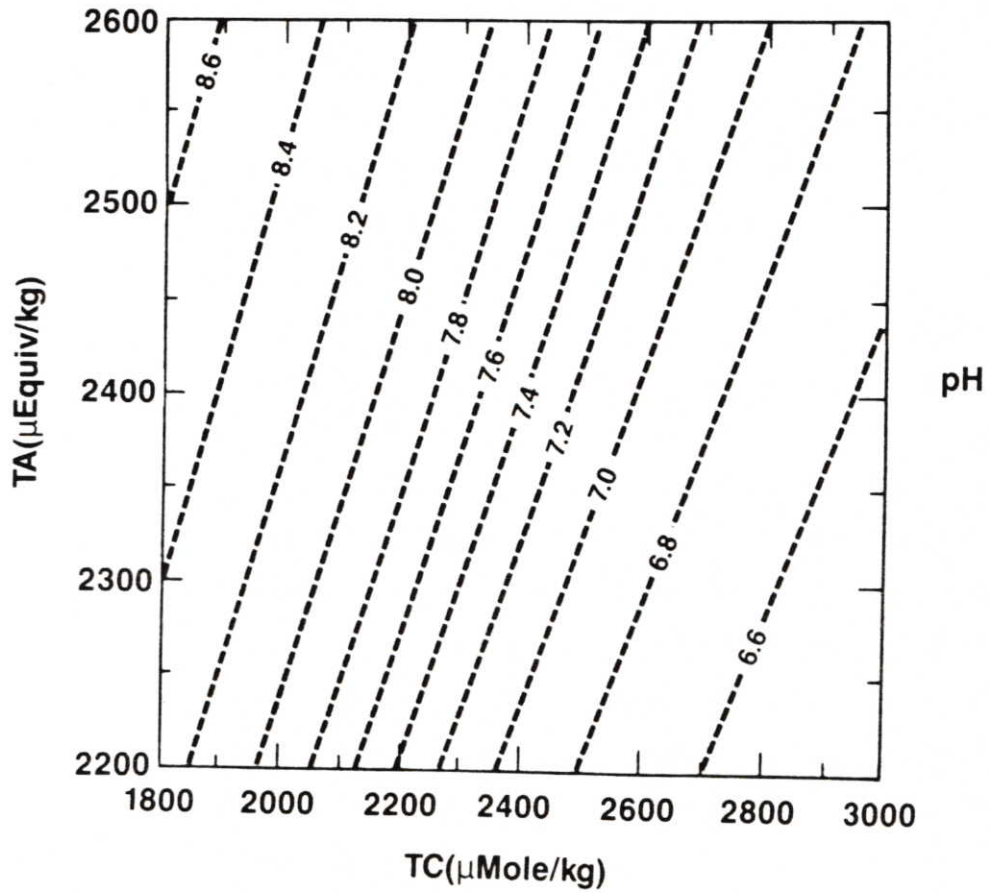
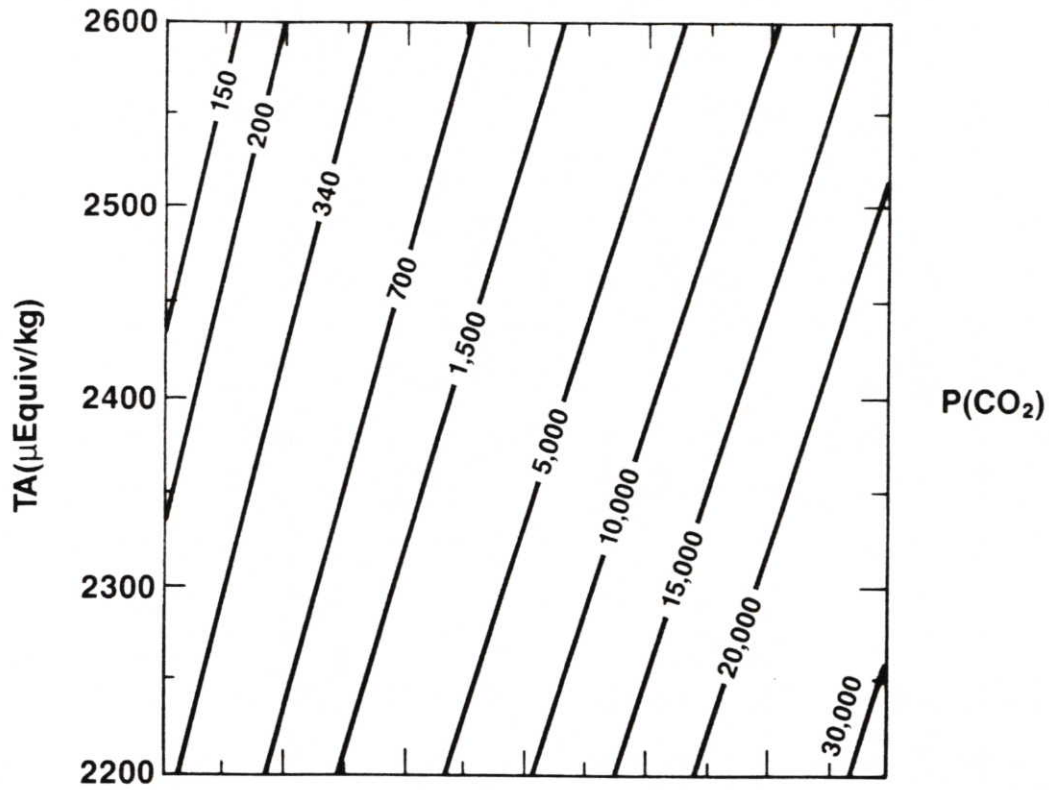
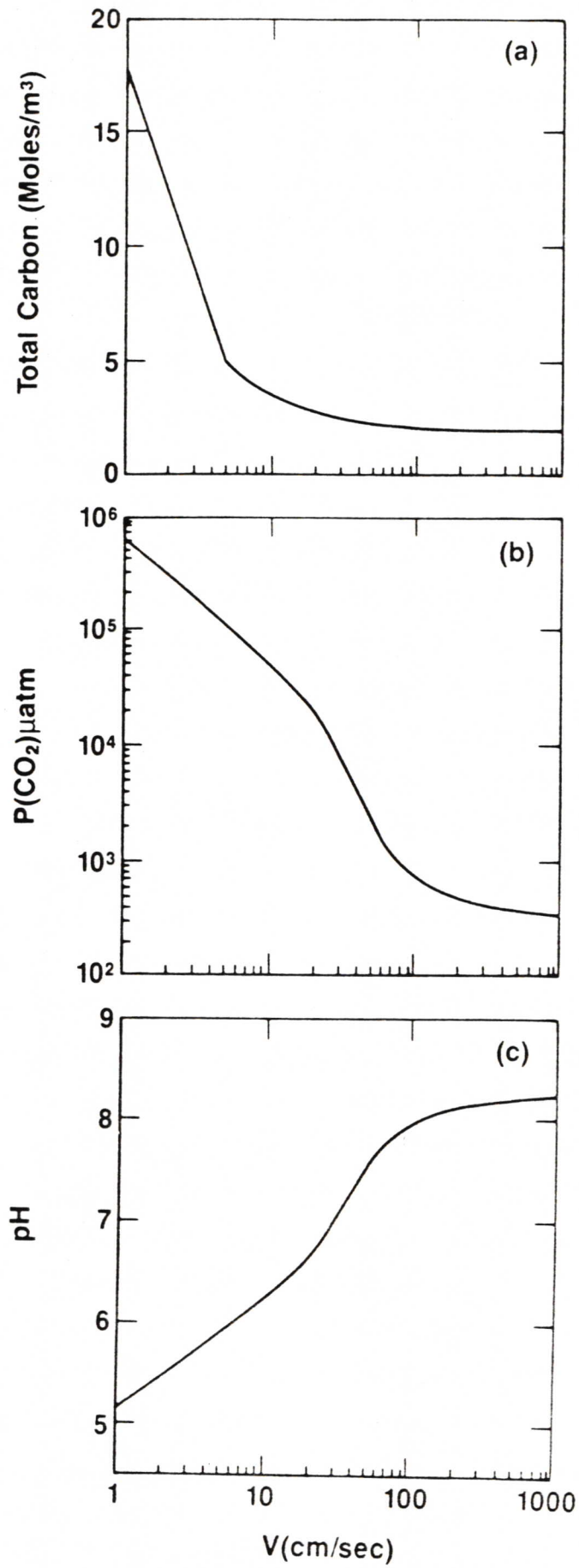


Figure 5



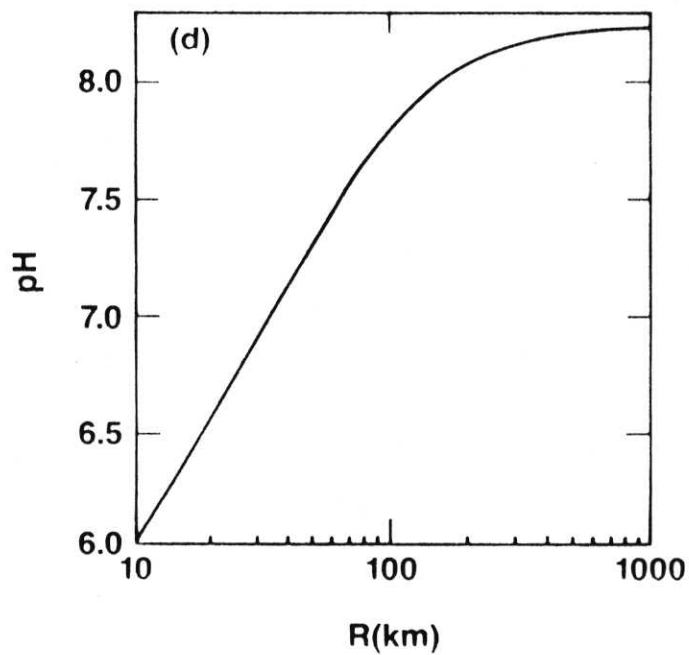
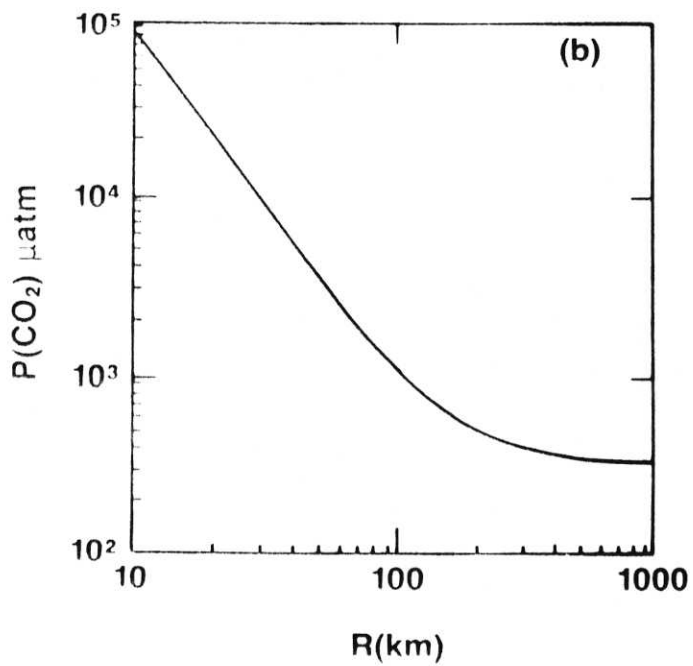
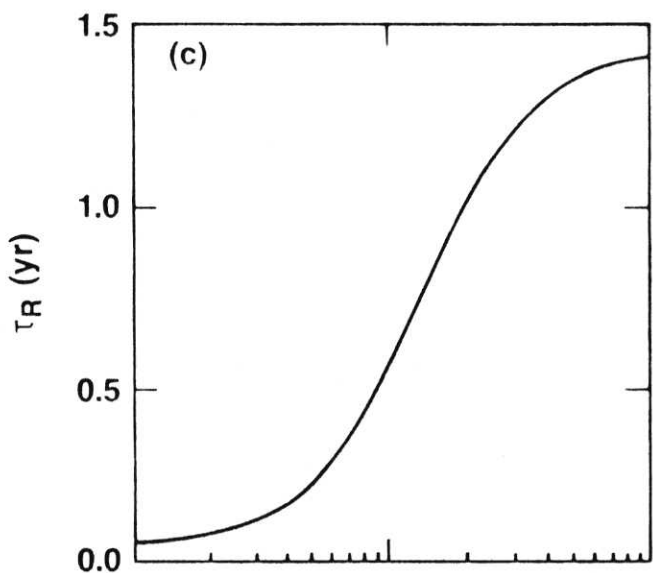
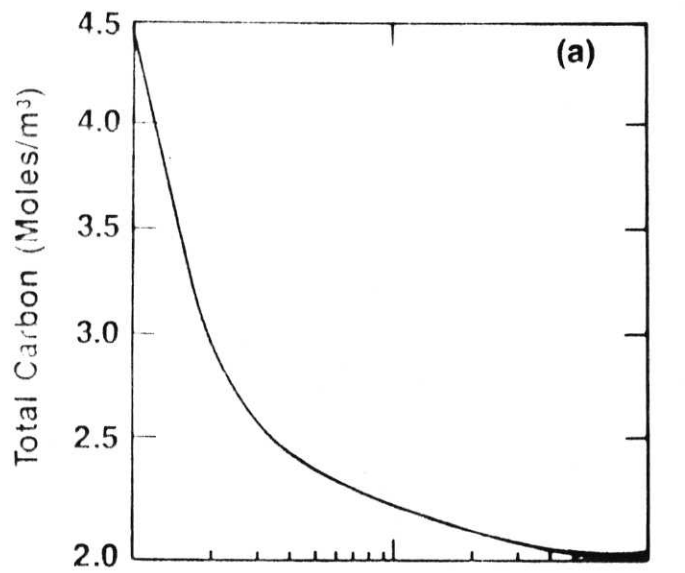


Figure 6

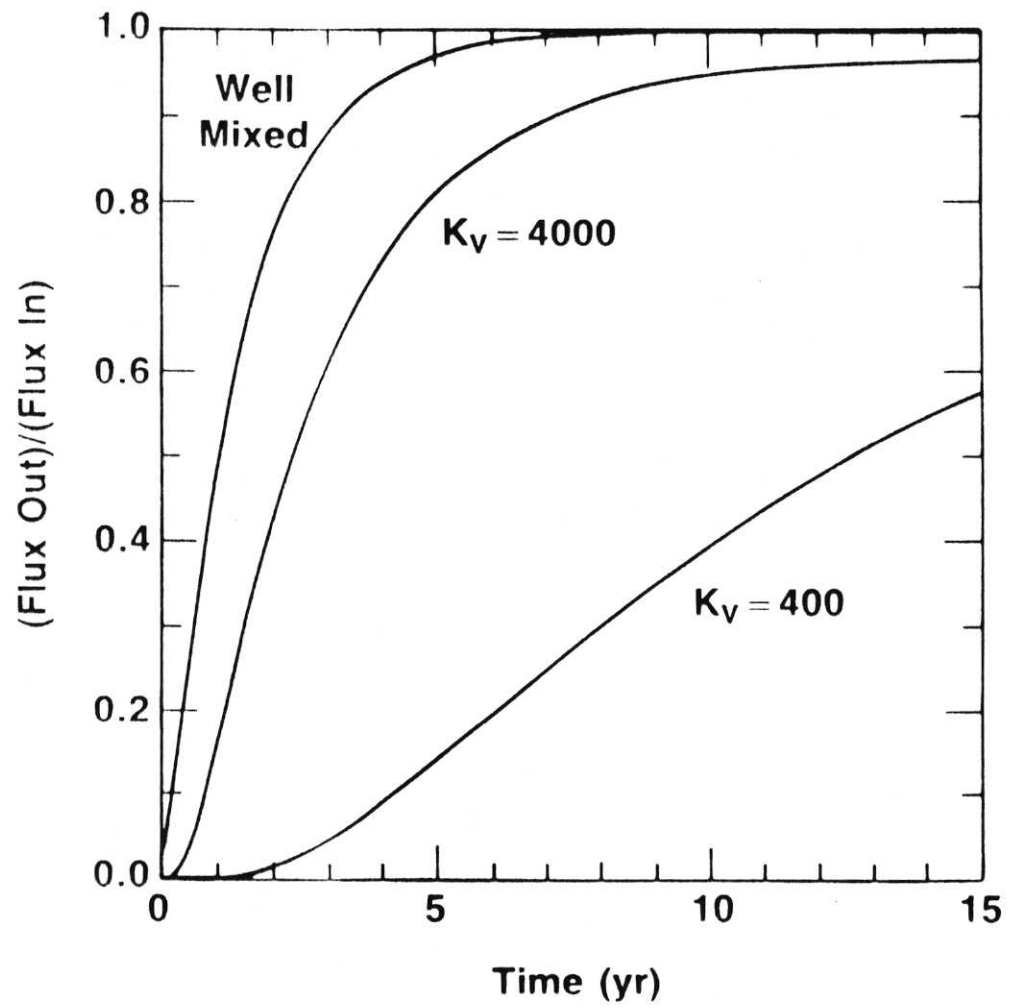
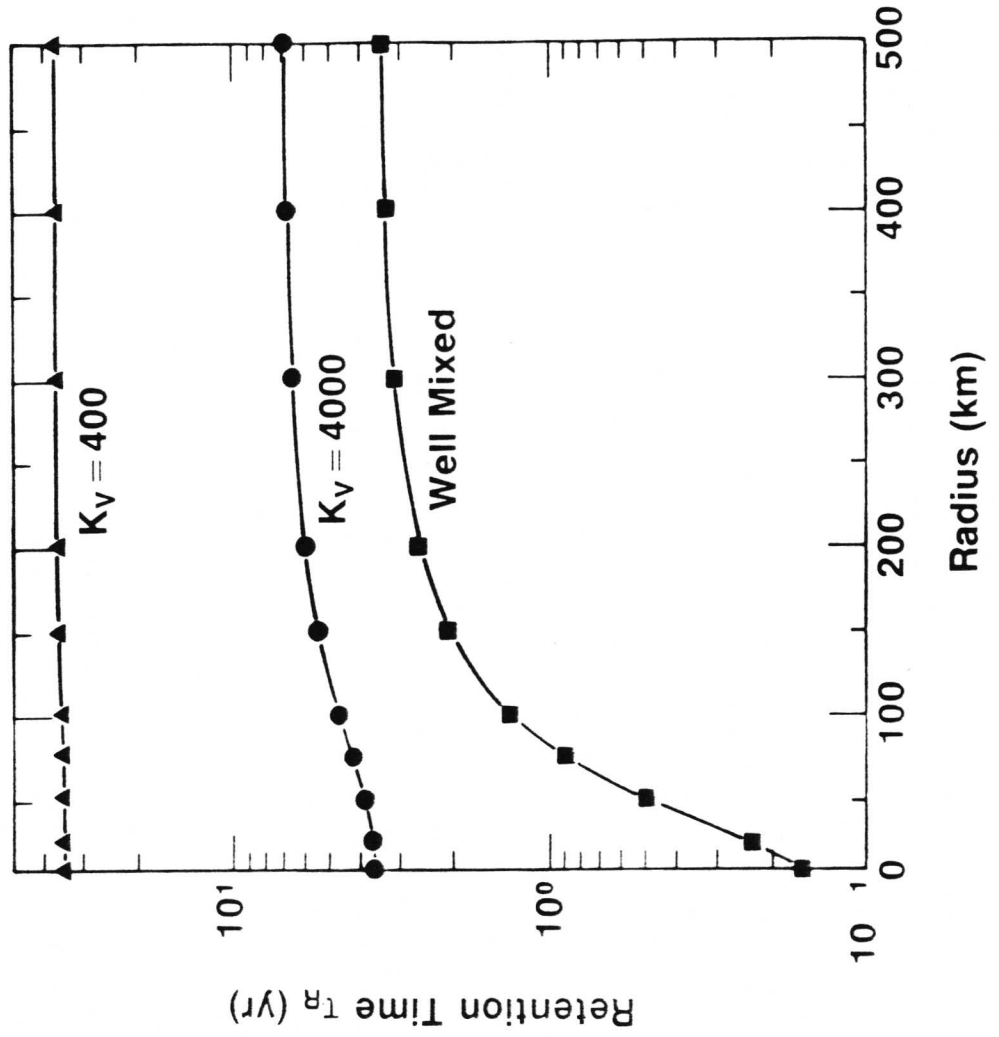


Figure 7

Figure 8



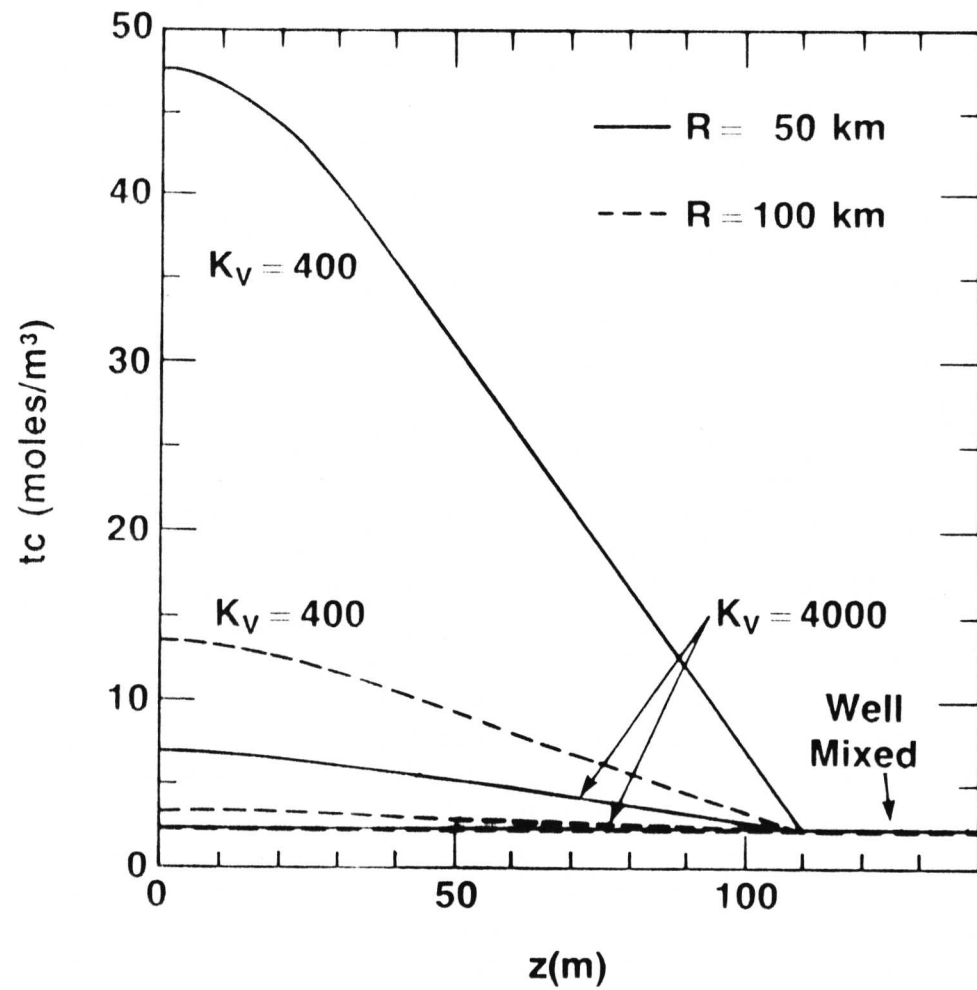


Figure 9a

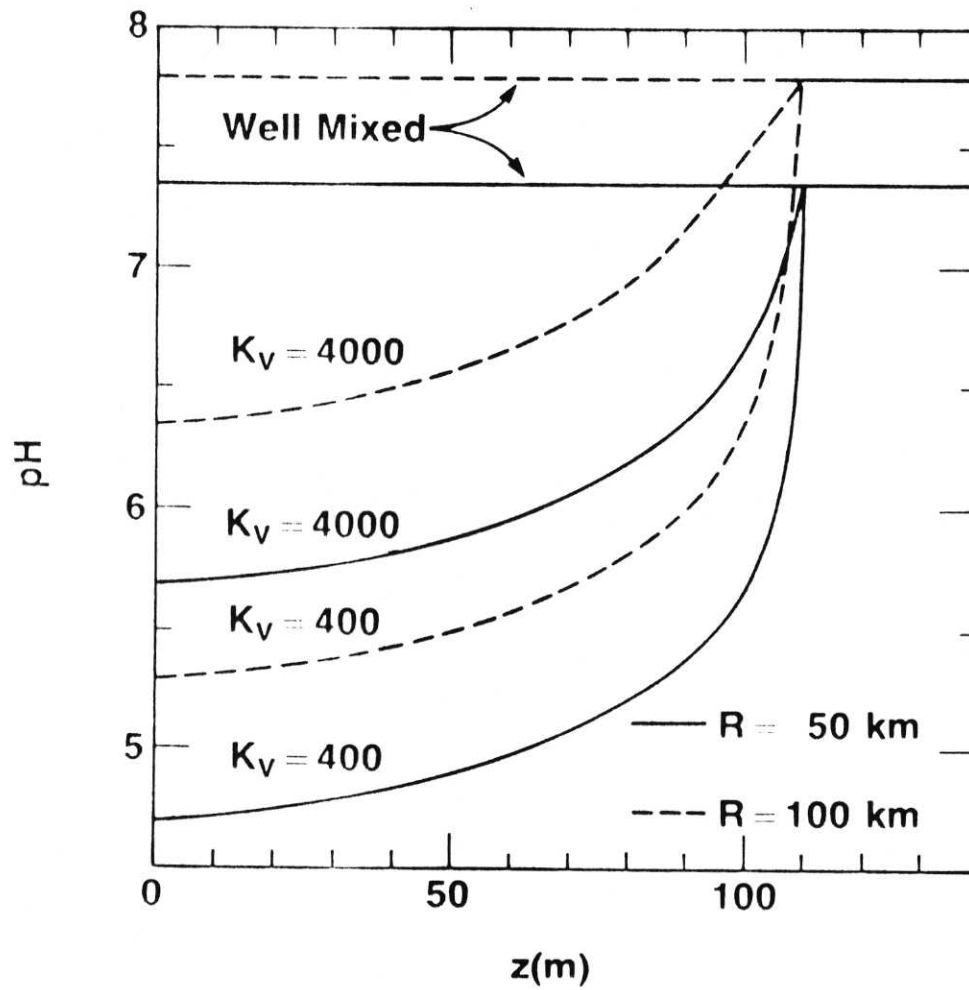
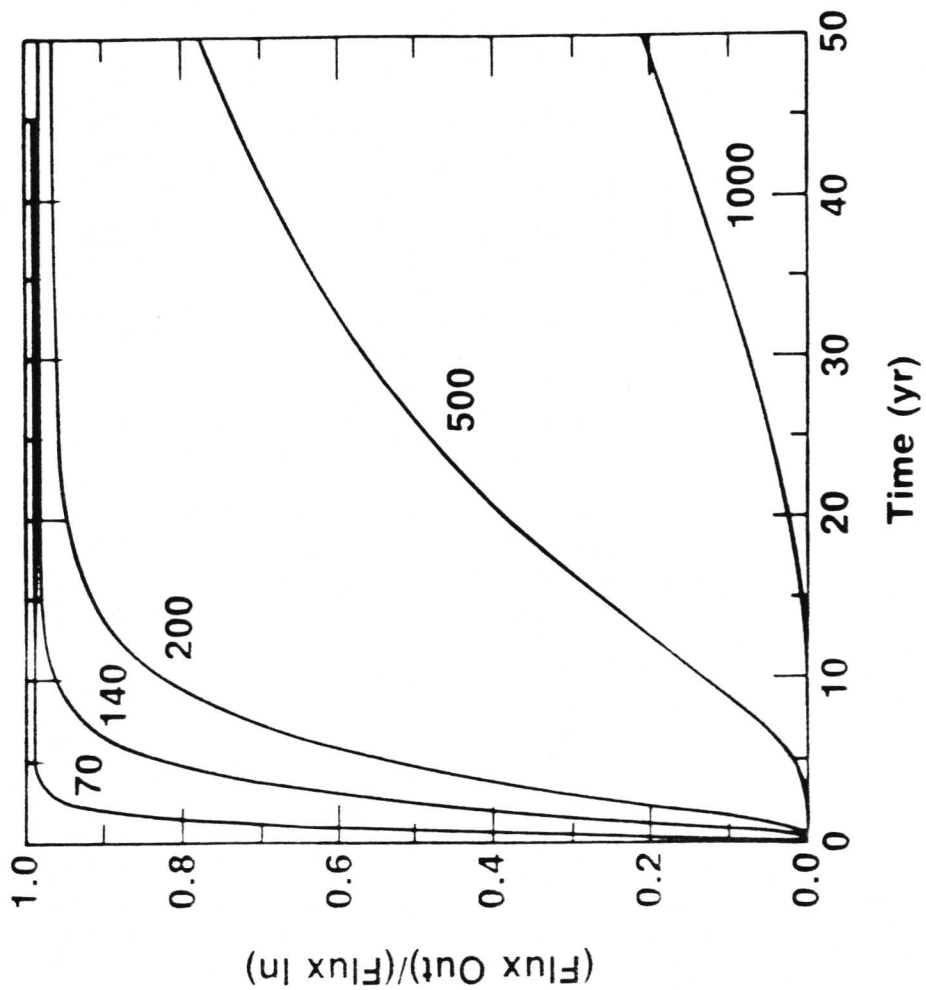


Figure 9b

Figure 10



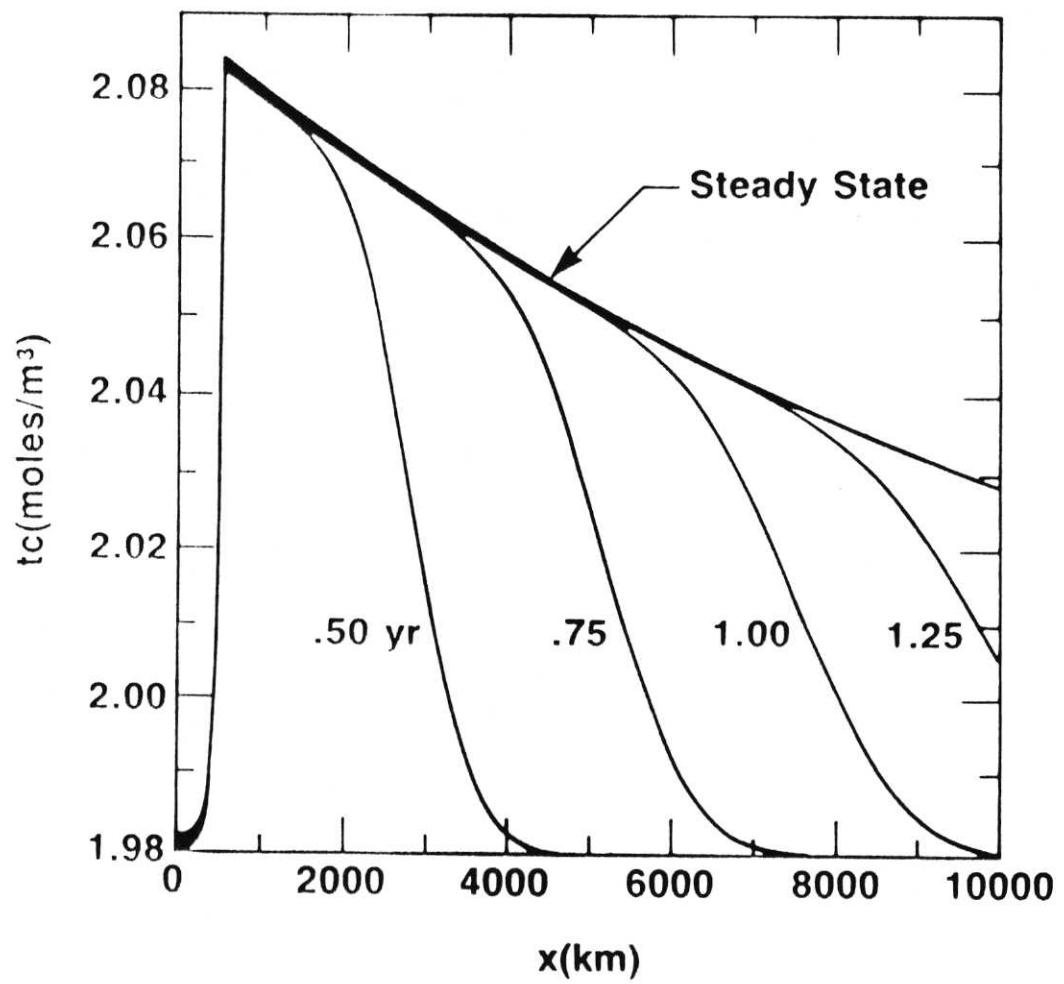


Figure 11a

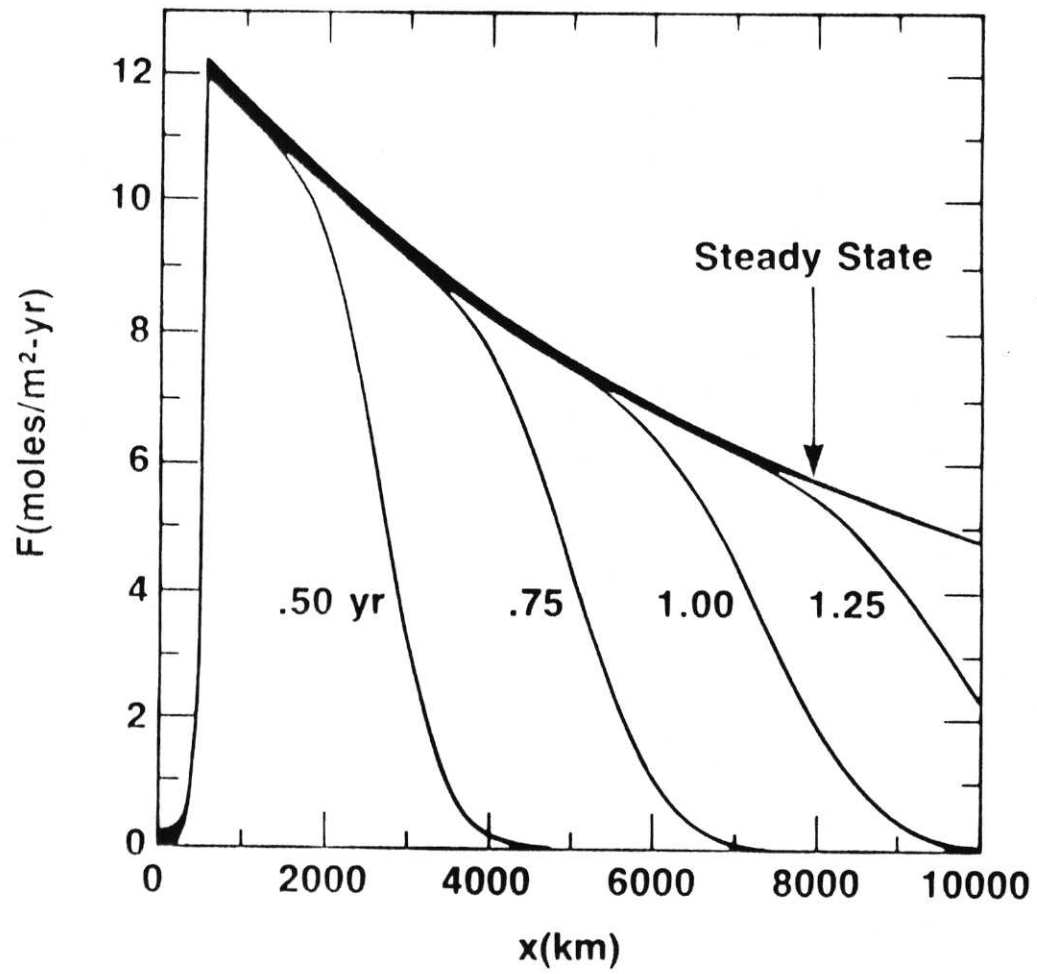


Figure 11b

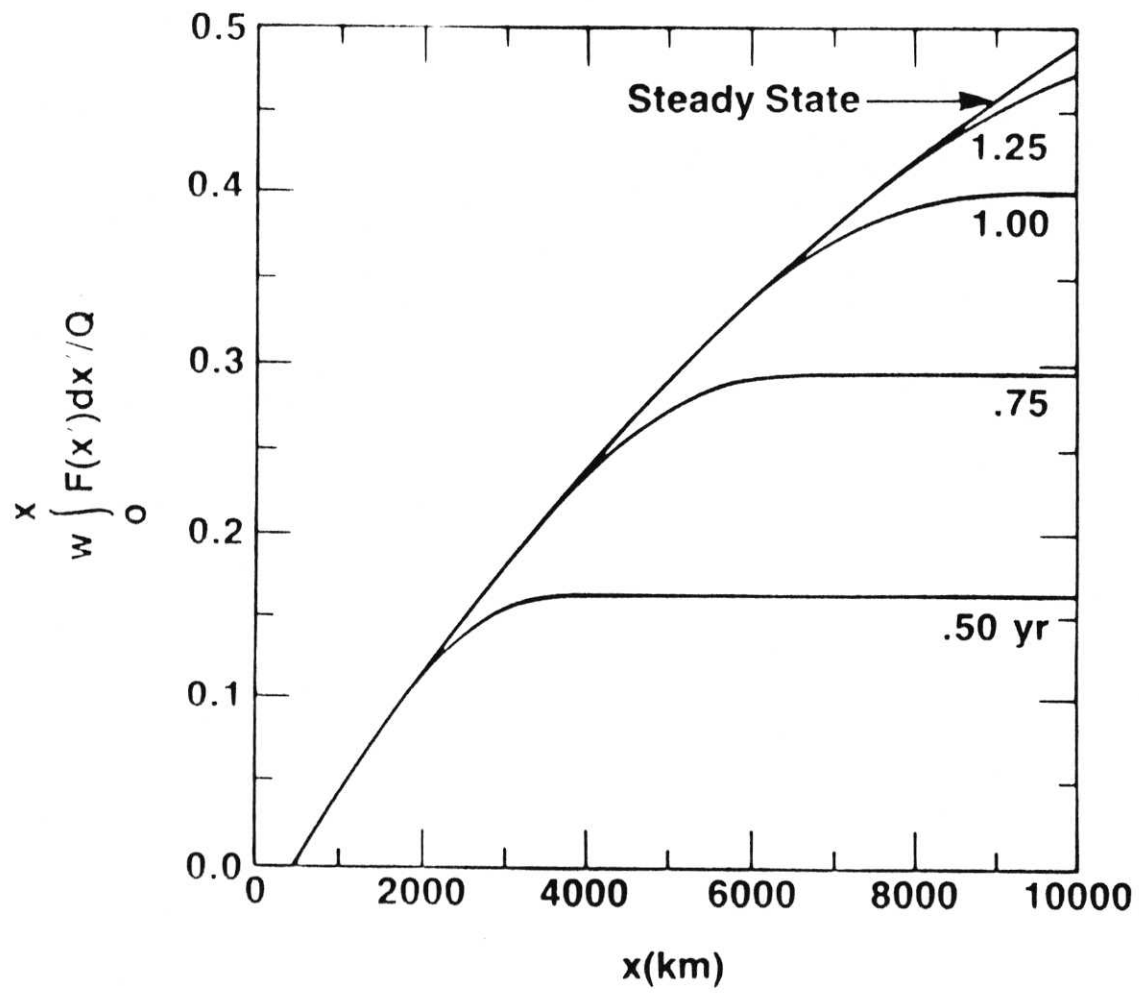
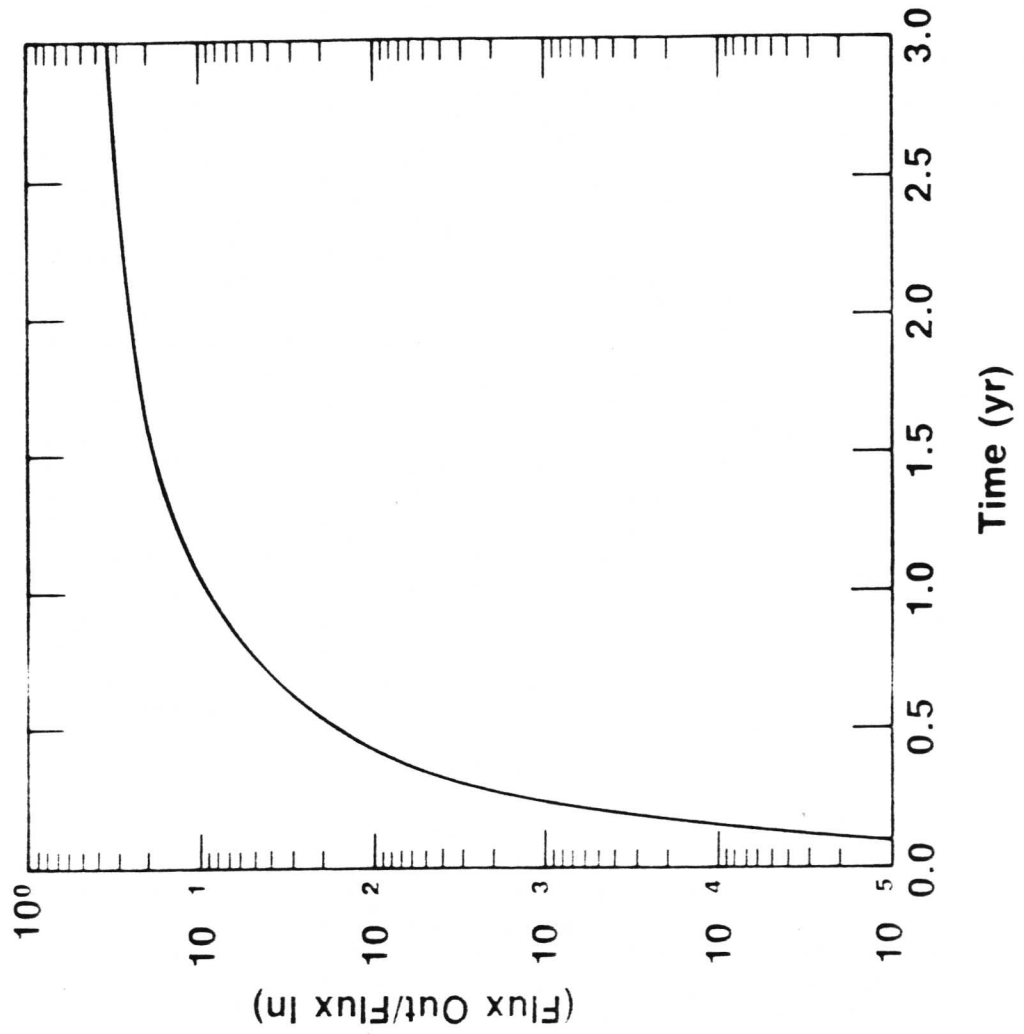


Figure 11c

Figure 12



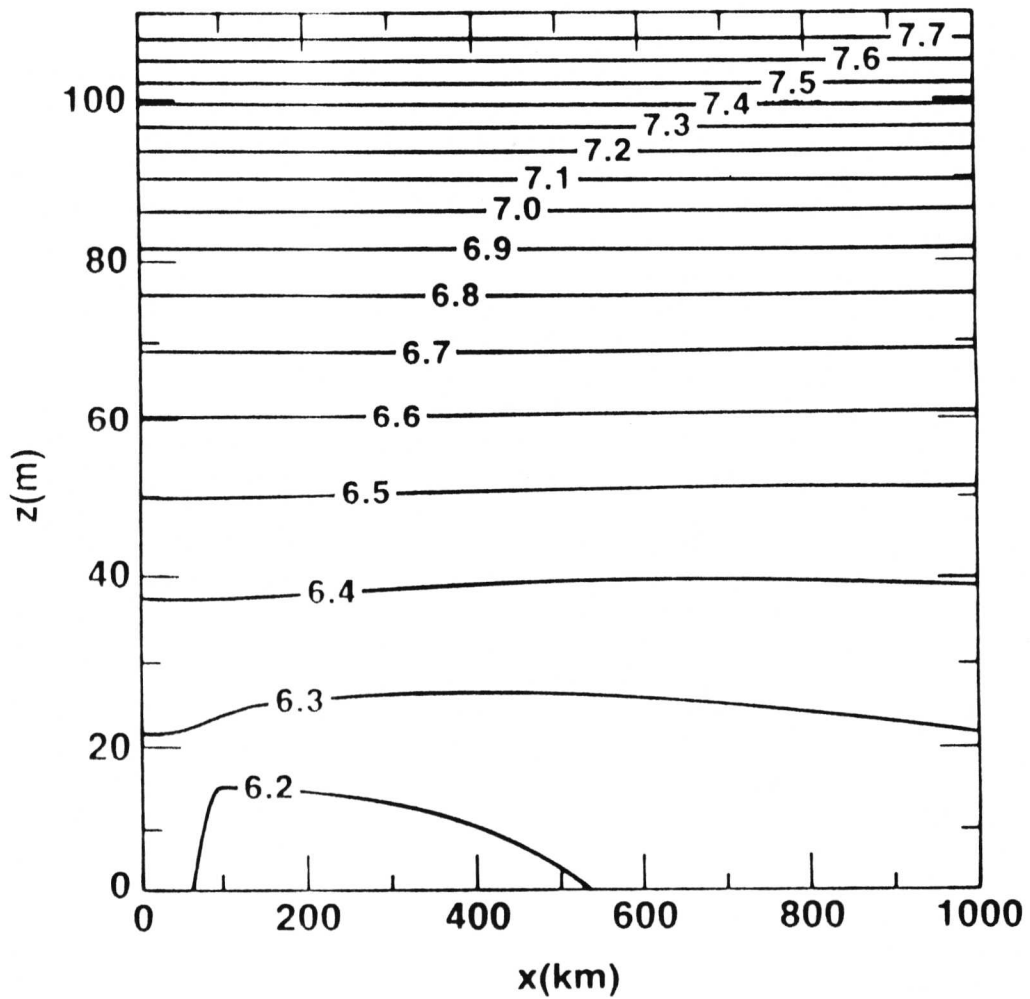


Figure 13

Figure 14

